Estimation of Water Table Depths and Local Groundwater Flow Pattern using the Ground Penetrating Radar

Manu E. [*], Preko K. [**], Wemegah D.D[**]

[*] Water Research Institute, CSIR Accra, Ghana
[**] Department of Physics, Kwame Nkrumah University of Science and Technology Kumasi, Ghana

Abstract- Estimation of groundwater table by hydrogeologists in Ghana over the past decades has proven to be difficult due to the dearth of data on piezometric heads from the very few boreholes present to access this data. The importance of this information in infrastructure planning therefore calls for the need to establish a precise geophysical method that can predict the depth to the water table at a relatively lower cost and higher efficiency as compared with prevailing conventional methods. This paper demonstrates how the ground based ground penetrating radar (GPR) has been successfully used to delineate water table depths and possible ground water flow directions. The MALA GPR equipment with unshielded rough terrain antenna of 25 MHz central frequency in the common offset mode was employed for the data collection. Data was taken along 21 profiles with inter-profile separation of 50 m over the study site of areal extent 1 km^2. Water table depths were estimated at an average depth of 21 m in an environment permeated by vertical structures which possibly served as pathways for groundwater infiltration. The general groundwater flow pattern was north-east in the northern and southern parts, and south-west at the central, eastern and western parts of the study area. The contact between the duricrust and the weathered saprolite was found at an average depth of 8 m. GPR-derived groundwater table depths were validated by drilled boreholes which intercepted the groundwater table at an average depth of 20 m within a lithology comprised of sandy clay and granite with varying degrees of weathering. This paper demonstrates the use of GPR as an efficient method for the estimation of groundwater table depth, groundwater flow direction as well as mapping of near surface lithological units; hence, it can serve as a baseline study for future applications.

Index Terms- GPR, water table, borehole, electromagnetic wave, groundwater, piezometric head.

I. INTRODUCTION

Groundwater has many hydrological applications. Management of irrigation, run-off, water resources and other agricultural practices depend to a wide extent on soil water content variability. Groundwater is an important source of potable water for both urban and rural communities in Ghana. Over the past decades the quest for groundwater has been on the increase since this often proves to be a more reliable source of drinking water than the easily contaminated streams and lakes. Most of the methods used to locate groundwater fonts include the electrical resistivity and time domain reflectometery. In the recent past, the ground penetrating radar (GPR) has come more into play. GPR is an electromagnetic method which has advantage over the conventional methods by being more affordable, fast and non-invasive. When the transmitting wave impinges on an object with varying electrical properties, part of the travelling wave gets reflected while part passes through the material. Some of the transmitted waves get absorbed by the material through which it travels. Due to attenuation caused by the materials electrical properties coupled with geometrical spreading, the wave finally dies off at a depth where the energy of the wave is not strong enough to be reflected. The depth of penetration and the strength of the reflected wave are mainly influenced by the electrical properties of the material such as the electrical conductivity and dielectric permittivity.

Literature shows enormous applications of the GPR technology in the hydrogeological field of studies. For example, the GPR method has been successfully used to delineate hydrogeological structures (Ziaqiang et al. 2009, Pilon et al. 1994, Singh 2005, Maria and Giorgio 2008, Overmeeren 1994, Kevin 2004, Dafflon et al. 2011, Sandberg et al. 2002, Milan and Haeni, 1991); clay layers (Gomez-Ortiz et al. 2010); ground subsidence (Nur and Saad 2013); hydrocarbon contaminated soil (Umar et al. 2008), Lake basin (Last and Smol, 2001). Other areas of GPR research include soil moisture measurements (Preko et al. 2009, Preko and Wilhelm 2012) environmental applications (Knight 2001; Denizman et al. 2008; Daniels et al. 1995), geological structural mapping (Ulriksen 1982, Eisenburger and Gundelach 2000, Franke and Yelf 2003, Slater and Niemi 2003, Da Silva et al. 2004, Leucci 2006), mineral delineation (Manu et al. 2013, Patterson and Cook 1999) and detection of water table at depth (Omolaiye et al. 2011, Ming-Chin et al. 2009, Thomas and Doolittle 1994, Doolittle et al. 2006 and Ismail et al. 2012) among several others. Geophysical exploration, especially with the use of GPR has highly enhanced the probability of locating successful drilling points in the quest for drinking water. This paper applies the GPR technology to delineate water table locations and possible groundwater flow patterns.

1.1 Principle of the GPR

The basic principle behind the GPR is the principle of scattering of electromagnetic waves. A short pulse of ultra-high frequency electromagnetic (EM) wave within the range of 1 to 5000 MHz is propagated through the earth. As the wave propagates through the ground, it encounters different earth materials of varying dielectric contrasts. Part of the wave energy

gets reflected and part transmitted through the material due to the bulk changes in the materials' electrical properties (e.g. relative permittivity (ε_r), magnetic permeability and electrical conductivity). The relative permittivity, a material property that controls the speed of the EM wave through material and the index of refraction is defined by,

$$\varepsilon_r = \frac{\varepsilon}{\varepsilon_0} \quad (1)$$

The propagation velocity v is related to the speed c of EM wave through vacuum and ε_r by

$$v = \frac{c}{\sqrt{\varepsilon_r}} \quad (2)$$

From equation (2), deductions can be made that, changes in subsurface material properties will cause a contrast in ε_r which will affect the index of refraction by producing a reflected energy at the boundary between two materials. The relative permittivity is mainly controlled by the soil water content. Increase in water saturation in a given formation will cause an increase in ε_r thereby increasing the energy of the reflected EM wave. The value of ε_r gives an idea of the type of soil hosting the aquifer zone. The propagation velocity v is calculated by

$$v = 2\frac{d_w}{t_w} \quad (3)$$

where d_w is the depth to water table and t_w is the two-way travel time to the reflector.

II. MATERIALS AND METHODS

2.1 Description of Project Site

The area under investigation is located between Teekyere and Adroba in the Tano district of Brong Ahafo Region and is about 300 km northwest of the capital of Ghana. Geographically, the study site is located on the geographical coordinate system of longitude 2°10'4.8" W and latitude 7°14'20.4"N **Figure 1**. The wet semi-equatorial climatic zone of Ghana prevails in and around the study area and is characterized by an annual maximum rainfall pattern occurring in the months of May to July and from September to October. The climate of the area is determined by movement of air masses which differ in air moisture and relative stability rather than temperature (Dickson and Benneh., 1970). Mean annual rainfall for the project area is between 1354 and 1400 mm. The minimal rainfall is experienced from December to the end of February, with January as the driest month. Mean monthly temperature within the area ranges from 23.9 to 28.4 ^{o}C. In general, March is the hottest month of the year with a mean temperature of 27.8 ^{o}C. August is the coolest month with a mean temperature of 24.6 ^{o}C (Dickson and Benneh., 1970).

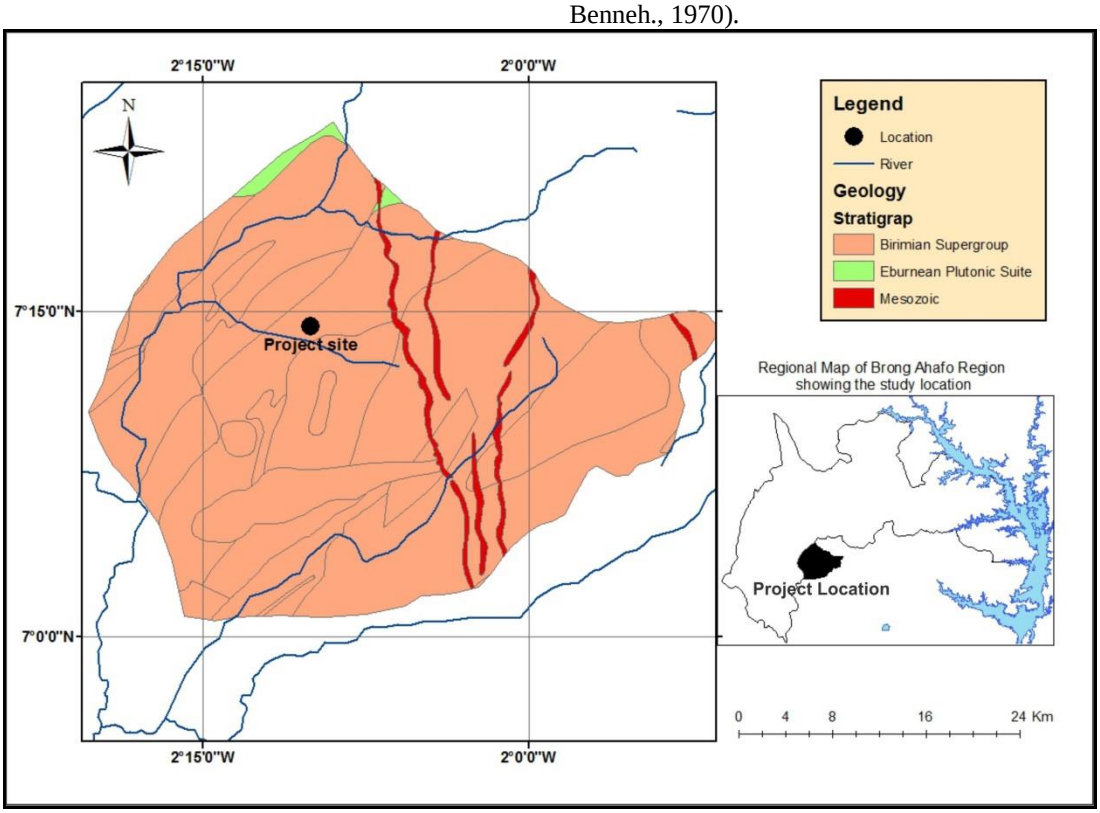

Figure 1 Geological map of the Tano District showing the location of the Study area

2.2 Geology Setting and Hydrogeology of the study Area

Geologically, the area lies within the Basement Complex (crystalline rocks), which underlies about 54 % of the entire land size of the country. The Basement Complex is further divided into subprovinces on the basis of geologic and groundwater conditions (Gill 1969). Generally, these subprovinces include the metamorphosed and folded rocks of the Birimian System and its associated granitoids, Dahomeyan System, Tarkwaian System, Togo Series, and the Buem Formation (Kesse 1985). The Basement Complex consists mainly of gneiss, phyllite, schist, and quartzite. The area under investigation falls within the Birimian subprovince of the Basement Complex **(Figure 1).** The Birimian system consists of great thickness of isoclinally folded, metamorphosed sediments intercalated with metamorphosed lava and tuff. The tuff and lava are predominant in the upper part of the system, whereas the sedimentary units are predominant in the lower part. The entire sequence is intruded by batholithic masses of granite. They are not inherently permeable, but secondary permeability and porosity have developed as a result of fracturing and weathering (Dapaa-Siakwan and Gyau Boakye, 2000). In some areas, weathered granite or gneiss formed permeable groundwater reservoirs. Major fault zones also were favorable locations for groundwater storage.

2.3 GPR Measurements

The GPR equipment used for the data collection is the MALA RAMAC GPR System with a Rough Terrain Antenna (RTA) system of central frequency of 25 MHz **Figure 2 (a).** The RTA antenna was ideal for the rugged nature of the study site. Data collection was done in the common offset mode. A total of 21 profile lines each of length 1 km and labeled T1, T2 …. T21 were surveyed on a 1 km square block **Figure 2 (c)**. The GPR setup was mounted and data collected by pulling the ruggedly designed RTA antenna along the profile lines at walking speed**.** Data was taken in the driest month (January) of the year when the water table was expected to be at its greatest depth. This was to help facilitate the delineation of structural features serving as conduit for water infiltration in the area. In this vein, GPR profile lines were set to traverse across the regional strike of lineaments which were aligned in the northeast-southwest (NE-SW) directions **Figure 2 (b).**

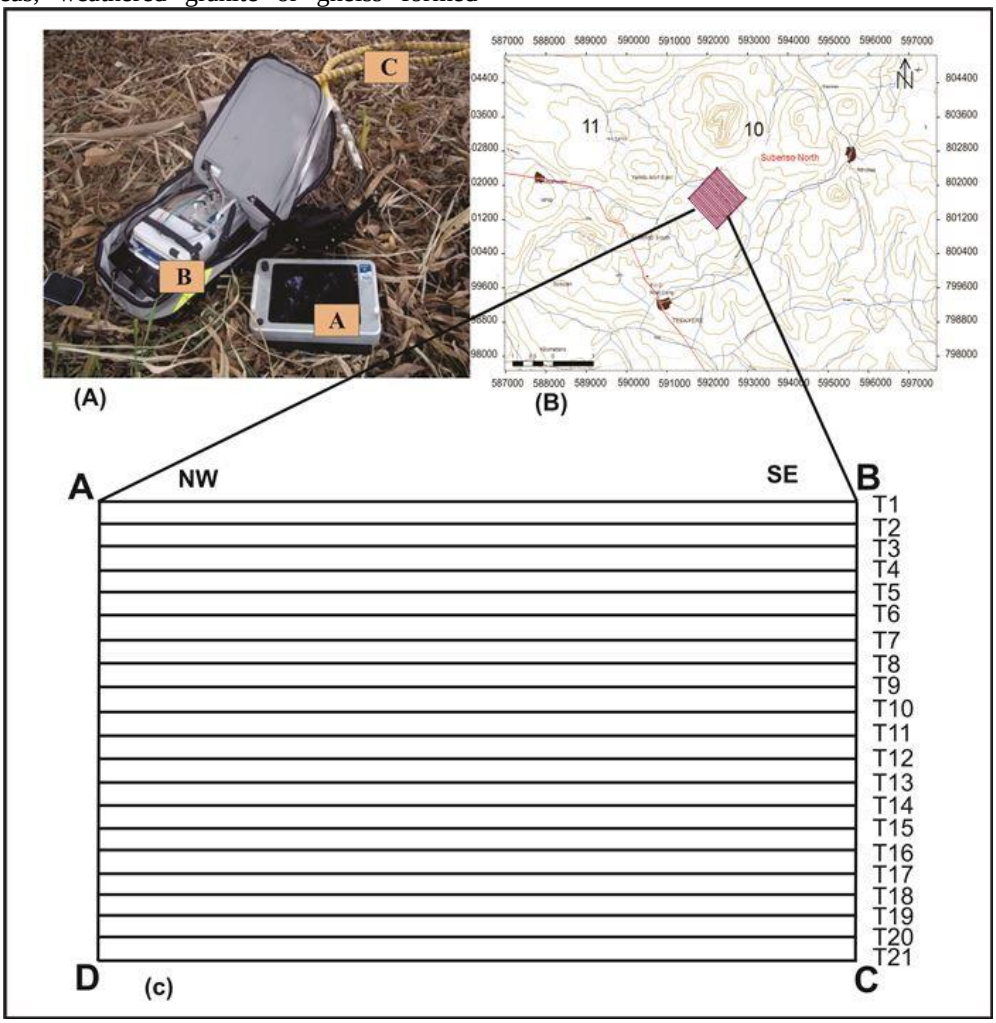

Figure 2 (A) MALA GPR equipment with A as XV monitor, B as control unit and C as Rough Terrain Antenna (RTA), (B) study location indicating northwest-southeast (NW-SE) orientation of 21 traverse lines and (c) expanded 1 km square grid of 21 traverse lines labeled T1, T2, …, T21.

2.4 Data Processing and Interpretation

Due to the large volume of the dataset, it was necessary to carry out data quality control to ensure good results. In view of this, the data obtained from the field were scrutinized by removing all bad data sets caused by unforeseen errors during data collection in order to ensure effective maintenance of the final data with the view of enhancing the signal to noise ratio. This was achieved after the raw data sets were processed with REFLEXW software (Sandmeier., 2012). The REFLEXW software made it easier to remove low frequencies from the data through the *dewow* tool. To resolve all traces to a common zero point, the *time zero correction* tool was activated on all the data sets to bring them to a fixed starting time. The *background removal* tool was further activated in the third step to temporarily remove coherent noise from the processed data. In order to enhance the signals received from the deeper depths, the *gain* tool was applied to enhance the drastic fall in energy of the wave before getting to the receiver.

2.5 Test Drilling of Borehole

Four borehole sites namely BH1, BH2, BH3 and BH4 were selected for test drilling to validate estimated water depths given by GPR and also to determine the geologic sequence underlying the study area. Drilling through the overburden at each location was done using 25-cm diameter roller bit to a depth of 7.5 m. This depth was subsequently protected from caving by installing a 7-inch diameter working casing. Beyond this depth, the drilling bit was changed to 6.5-inch diameter drilling hammer, and using air as the drilling fluid. Drilling continued with the hammer until drilling terminated at a final depth of 70 m. During the drilling process, logging and sampling of the drilling cuttings were made at 1 m intervals. This was to identify the precise fracture sections and the exact water strikes with depth. The water-bearing zones (aquifer sections) were recorded as drilling continued in order to ascertain the various water surfaces present.

III. RESULTS AND DISCUSIONS

The GPR signal from groundwater table (surface) could be due to the reflection caused by the strong dielectric contrast between the saturated and the unsaturated zones within the earth or the phase shift between the transmitted and the reflected signal (Shih et al. 1986, Daniel et al. 1995). All the radar sections analyzed had reference to these factors. Water table discussions in this paper are limited to the prevailing situation observed in January 2012 due to the periodic fluctuating nature of the water table. The month of January was chosen for the field work because it is the driest month of the year when the ground water table was expected to be at its greatest depth. Figures 3 and 4 represent 8 radar sections labeled T1 to T8. These radargrams mark a clear distinction between two lithological units, the saprolite and duricrust. The contact D between the two units occurs at a depth of about 8 m. The horizontal surface marked W indicates the water table. The radargrams show repeated hyperbolic reflections that indicate possible vertical fractures serving as conduits to facilitate ground water ascension. On the other hand, the water table depth is interpreted as the water saturated zone with highest dielectric contrast. This is mapped as horizontal continuous reflector seen at the depths of 23 m for T1, 21 m for T2 and T3 and 22 m for T4. From these depth values, the average water table depth was estimated at 22 m. Table 1 shows the relative dielectric permitivities of the unsaturated regolith overlying the water table. The average ε_r value of 9 for the regolith indicates a possible fractured and wet granitic rock. Figure 5 shows the contour plot of the water table. The lowest water table depth from the contour plot is about 18 m while the highest is about 26 m. The water table surface showed a descend from 24 m to 20 m between the traverse intervals of 200 m and 600 m and 24 m to 22 m for traverse intervals 800 m to 1000 m. These changes in depth in groundwater table gave possible flow directions of the groundwater resource. This incident also suggested a possible northward flow direction in most parts of the study area.

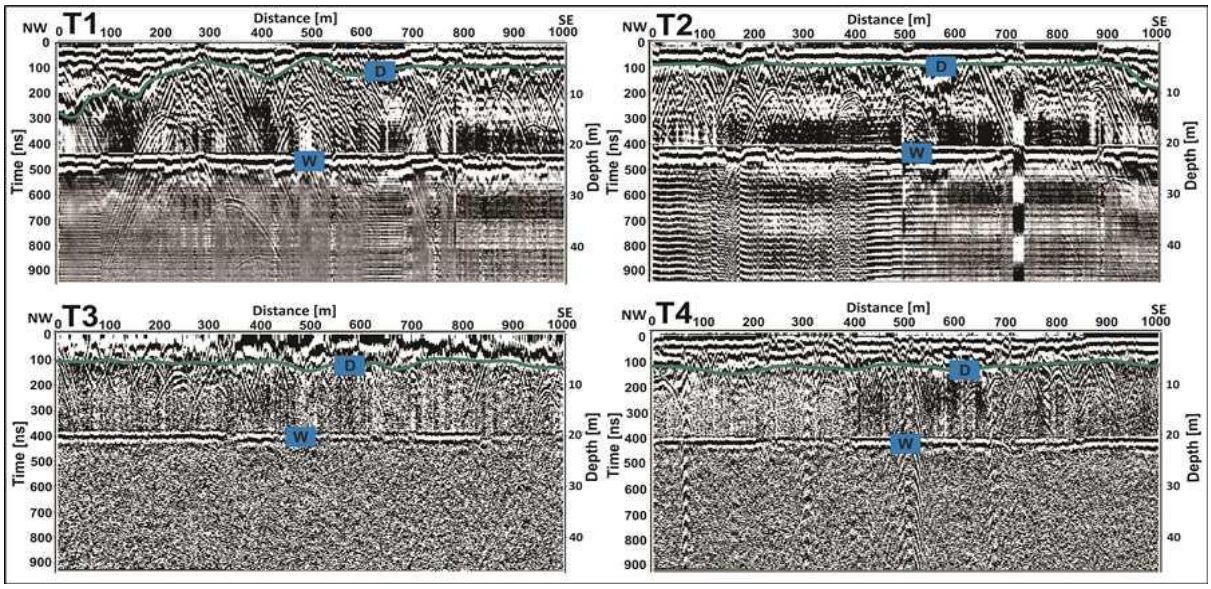

Figure 3 Radar sections for traverses T1, T2, T3 and T4

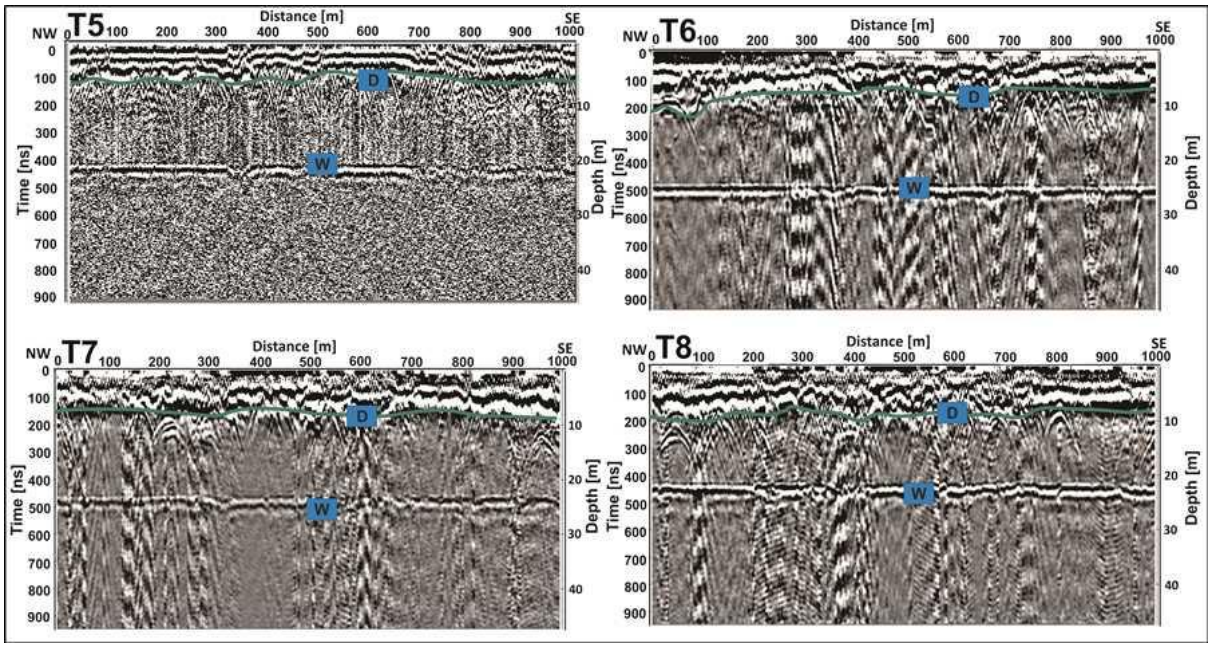

Figure 4 Radar sections for traverses T5, T6, T7 and T8

Table 1: Dielectric constant (ε_r) calculation for various profiles

T1	T2	T3	T4	T5	T6	T7	T8
8.6	9	9	9	9	9	9.4	8.4

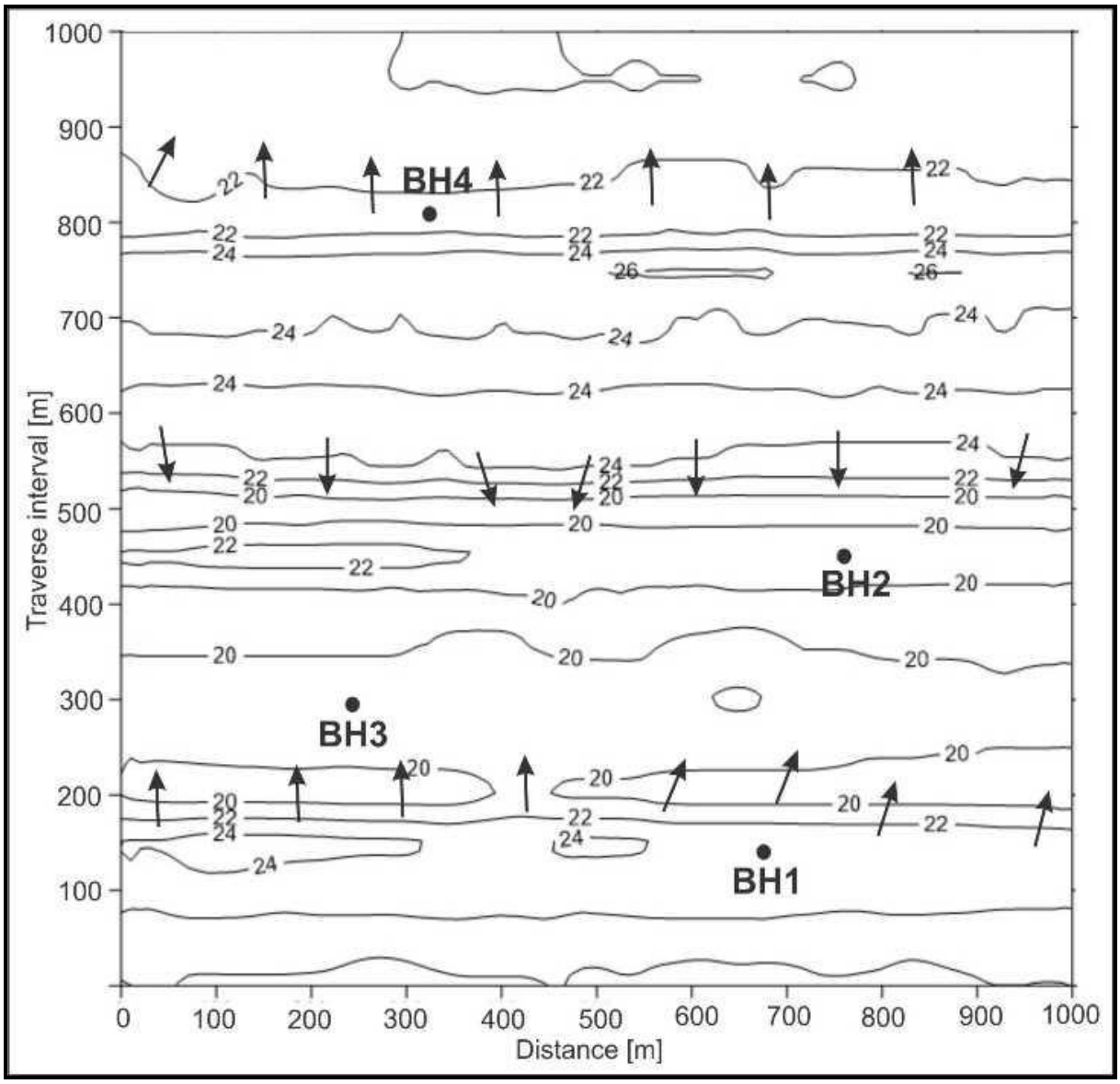

Figure 5 water table or potentiometric surface map from the GPR data

3.1 Correlation of Geophysical and Drilling Results

Four (4) boreholes BH1-BH4 were drilled at selected points to validate the results of the GPR measurements on the depths of the water table and the expected groundwater flow directions. The drill logs of the boreholes are shown in Annexes 1, 2, 3, and 4, indicating the various water strikes representing the water table. The GPR measurements estimated the water table to an average depth of 21 m which was within the range of 18 m and 24 m deduced from the drilled boreholes within highly weathered granitic rocks.

3.2 Error Estimation

Jol (2009) established that, the depth to water table can be defined in terms of propagation velocity v and two-way travel time t_w as $d_w = \frac{1}{2} t_w v$ where d_w is the depth to the water table while t_w is the two-way travel time. The random error in d_w is given by $\Delta d_w / d_w = \Delta t_w / 2t_w + \Delta v / 2v$. Several exercises of estimating the average two-way travel time t_w and the ground wave propagation velocity v gives $\Delta t / t \approx 2\ \%$ and $\Delta v / v \approx 4\ \%$. This means that for the maximum estimated water table depth $d_w = 24$ m, $\Delta d \approx 24/2[6\%] \approx 0.72$ m.

IV. IMPLICATIONS OF THE MEASURMENTS

GPR has been tested over some decades now by researchers in the Geoscience fraternity. This method has gained grounds and is well established in the geophysical arsenal for the imaging of the subsurface. In more favorable terrains where conductance is low especially in hard granitic environments, the GPR is

incomparable in the wealth of detailed subsurface mapping. In GPR applications, the reflected signal is caused mainly by the contrast in the relative dielectric permittivities of the traversed rocks. Different earth materials differ in their dielectric constant (ε_r) values depending on the amount of water they contain. Water is known to have the highest ε_r of about 81. Materials containing water produce strong reflections in the transmitted EM wave. The water table which is a contact between the saturated and unsaturated layers was seen in the radargram as a horizontal strip.

ANNEXES

Annex 1: Borehole construction profile for BH1

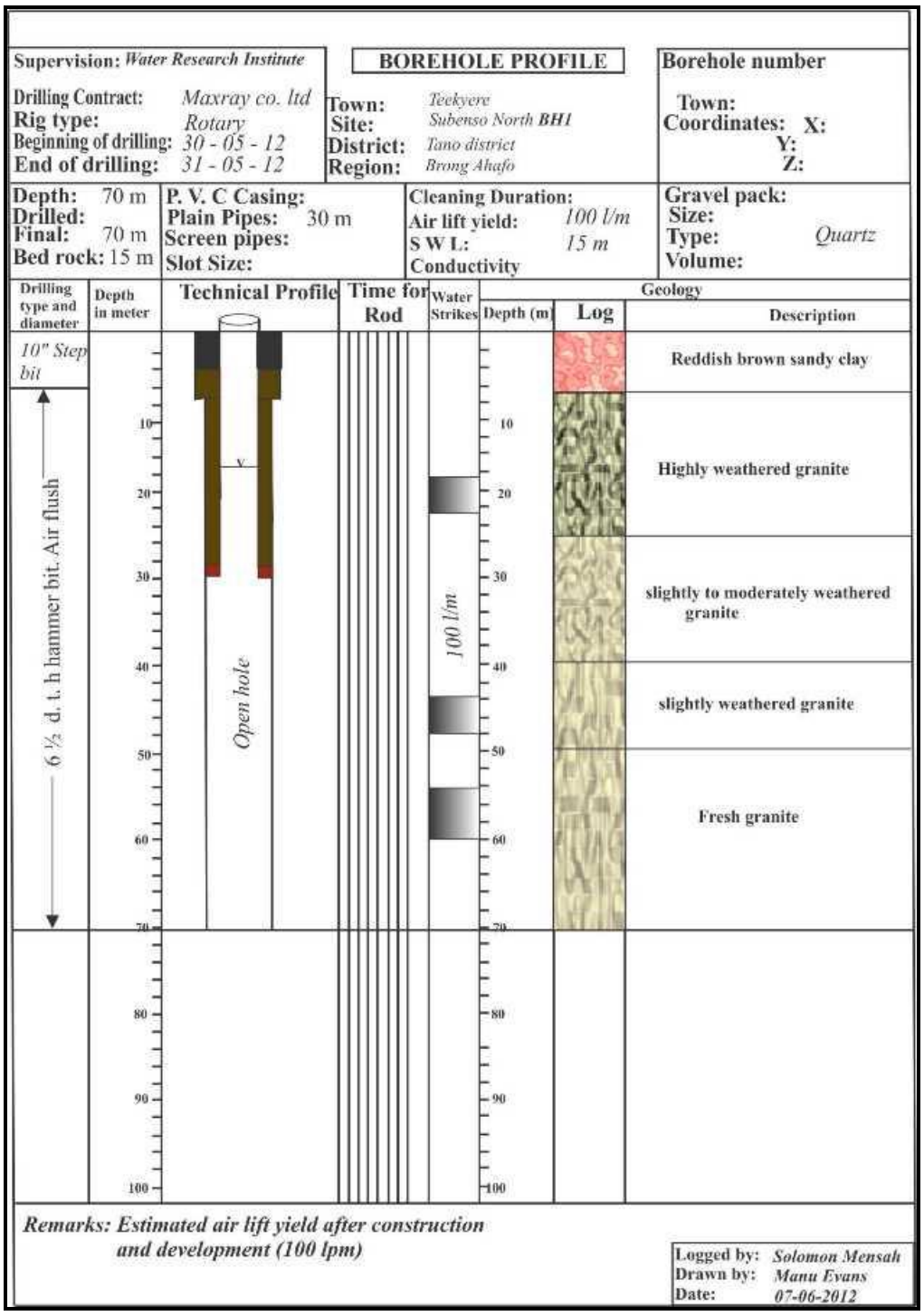

Annex 2: Borehole construction profile for BH2

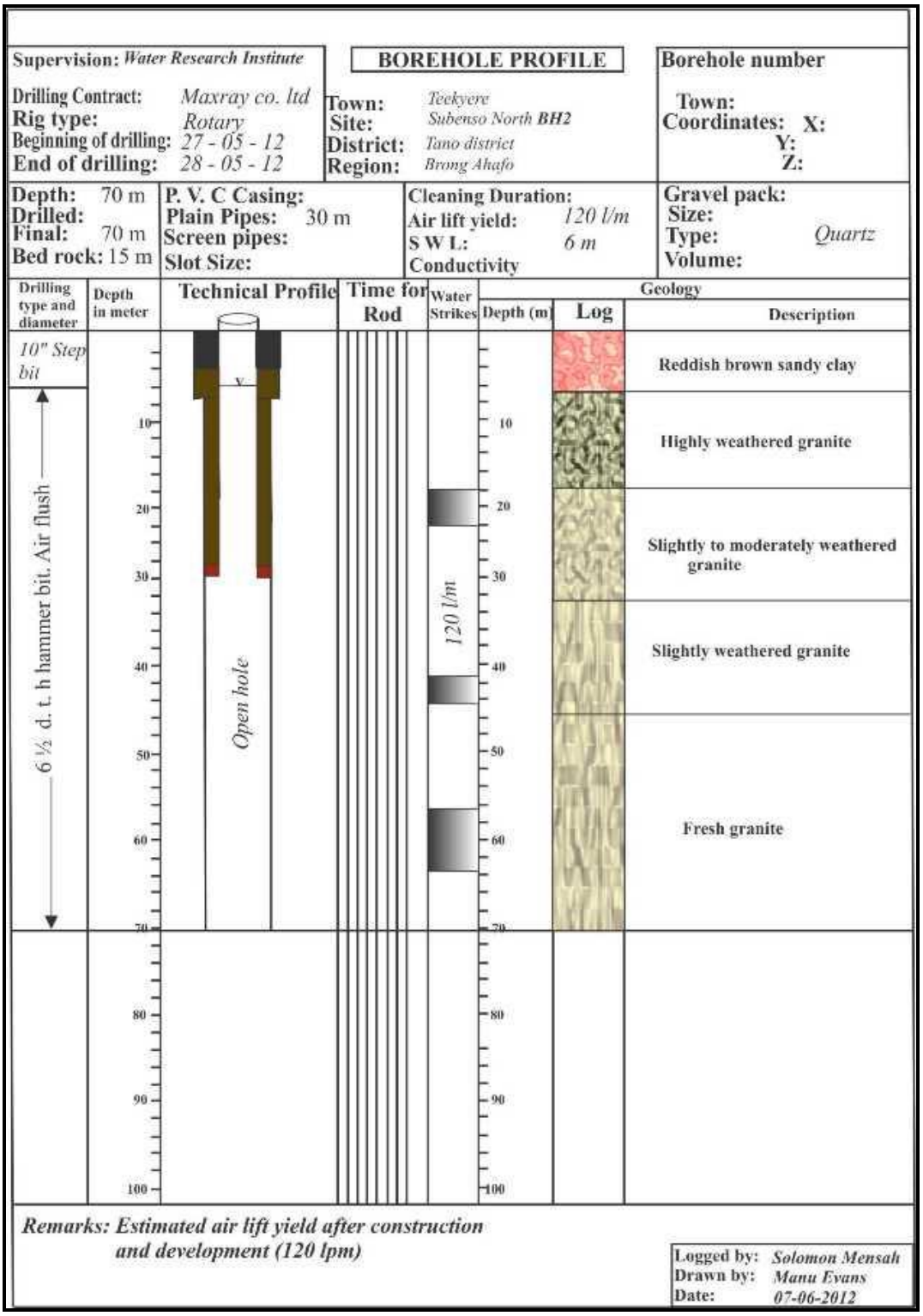

Annex 3: Borehole construction profile for BH3

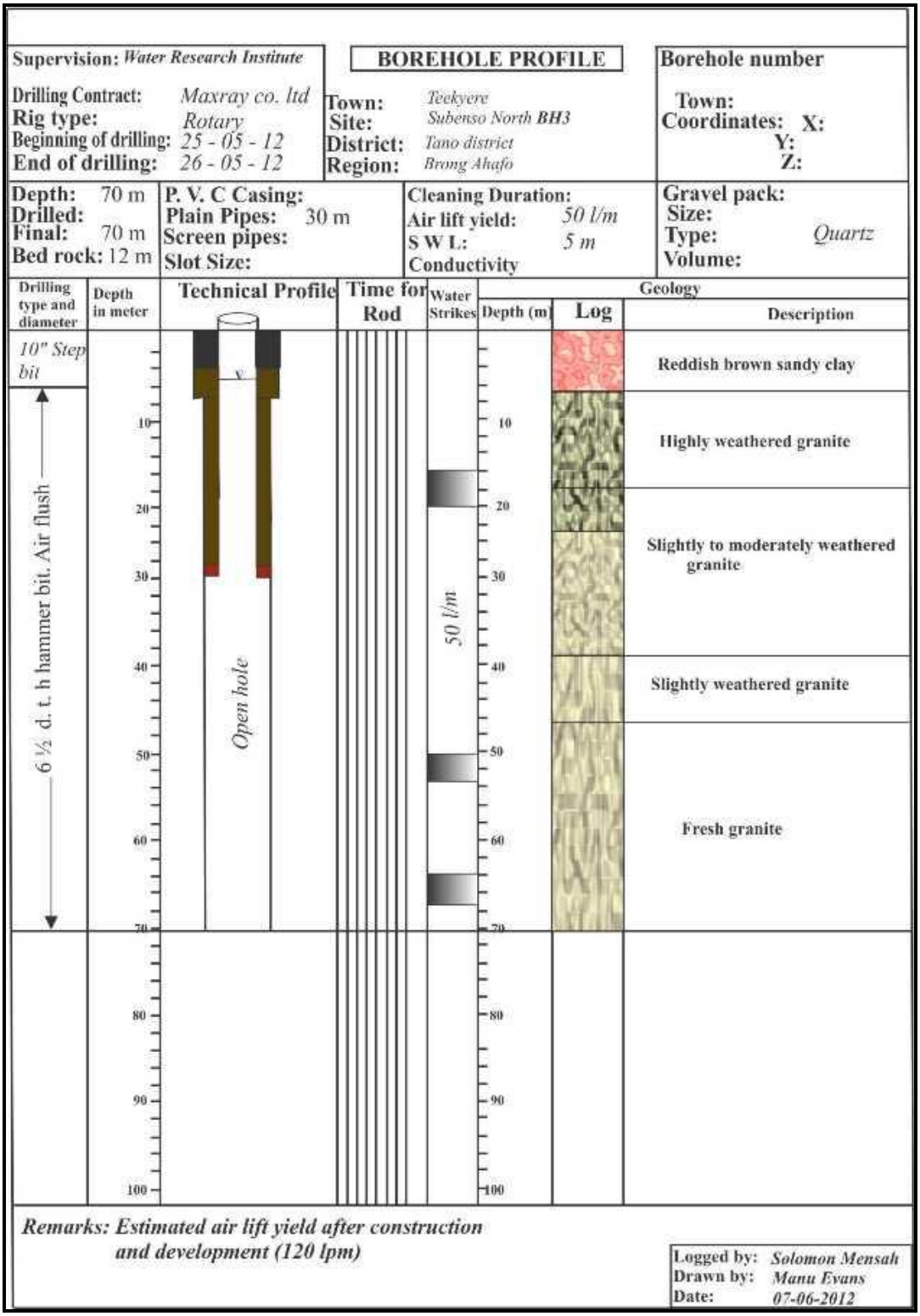

Annex 3: Borehole construction profile for BH3

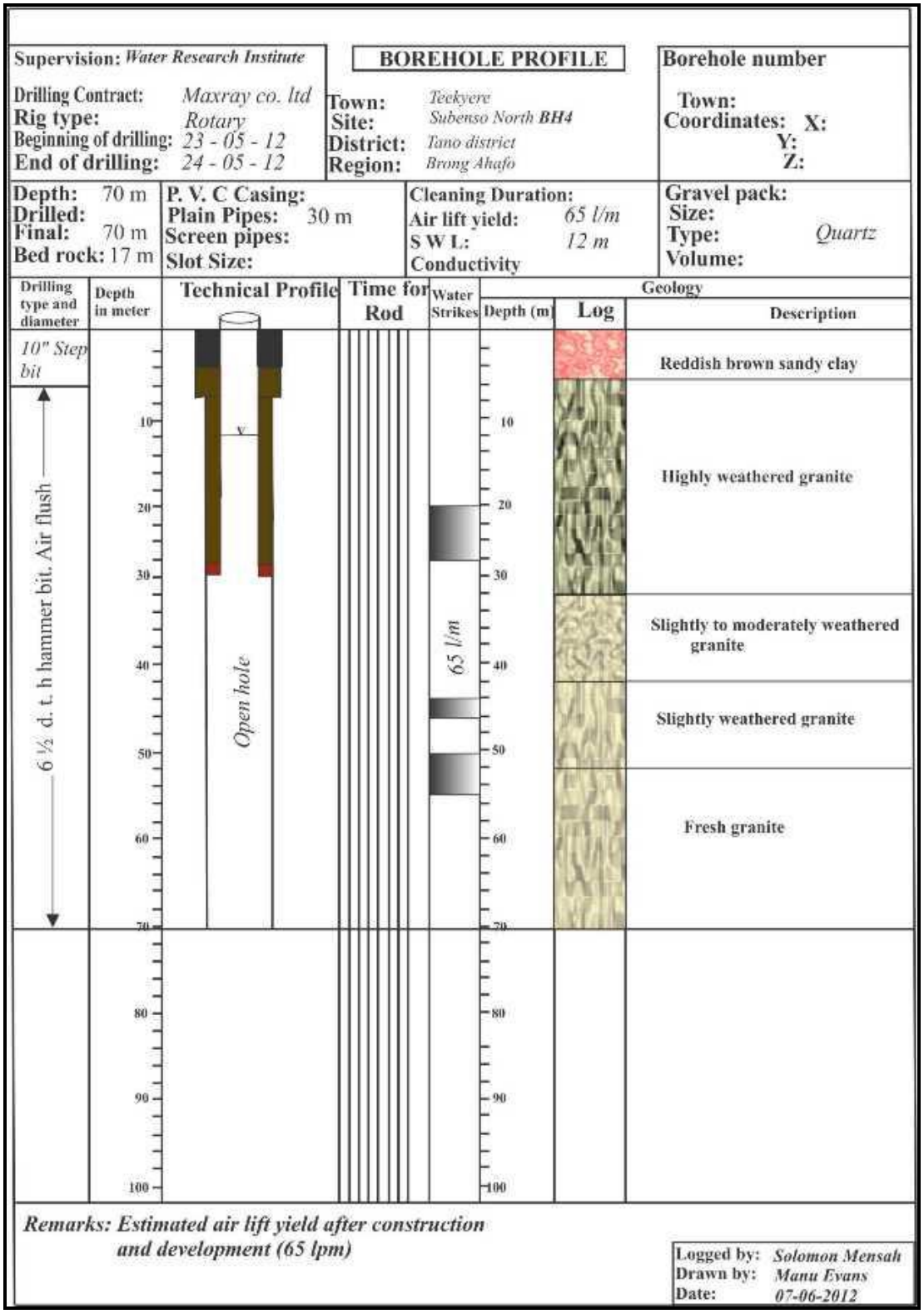

ACKKNOWLEDGMENT

This study was partially supported by Newmont Ghana Gold Limited with Kwame Nkrumah University of Science and Technology Physics Department as the main collaborative institution. We are grateful to Mr. Thomas Tsiboah and Mr. Kwaku Takyi Kyeremeh all at Newmont geophysics section. We also express our heartfelt gratitude to all our field personnel and also to lecturers in the Physics Department of KNUST for their

constructive criticism toward this study. We are most grateful to all that matter.

REFERENCES

[1] C.C.N. Da Silva, W.E.de Medeiros, E.F. Jardim de Sa and P.X. Neto, 2004. Resistivity and ground penetrating radar images of fractures in a crystalline aquifer. A case study in Caicara farm - NE Brazil. Journal of applied geophysics, 56.

[2] B.J. Dafflon Irving and W. Barrash, 2011. Inversion of multiple intersecting high – resolution crosshole GPR Profiles for hydrological characterization at the Boise hydrogeophysical research site. Journal of applied geophysics 73 (2011) 305 – 314.

[3] S. Dapaa – Siakwan, and P. Gyau _ Boakye, 2000. Hydrogeologic framework and borehole yields in Ghana. Hydrogeology journal (2000) 8:405 – 416.

[4] J.J. Daniels, R. Roberts, M. Vendl, 1995. Ground penetrating radar for the detection of liquid contaminants. Journal of applied geophysics, vol. 33, no. 33:195 – 207.

[5] K. Dickson, and G. Benneh, 1970. A new geography of Ghana. Metricated edition.

[6] C. Denizman, E.C. Brevik and J. Doolittle, 2008. Ground penetrating radar investigation of a rapidly developed small Island in a Lake in Southern Georgia, USA, Journal of Cave and Karst studies, vol. 72, no. 2, pp. 94 – 99. DOI: 10:4311/jcks 2008cs0060

[7] J.A Doolittle, B. Jenkinson, D. Hopkins, M. Ulmer and W. Tuttle, 2006. Hydropedological investigations with ground penetrating radar (GPR): Estimating water – table depths and local groundwater flow pattern in areas of coarse – textured soils. Geoderma 131 (2006) 317 – 329.

[8] D.M. Eisenburger, and V. Gundelach, 2000. Borehole radar measurements in complex geological structures. Proceedings of 8th internal conference on ground penetrating radar, SPIE 4084, April 27, 2000, pp: 21.

[9] J.C. Franke, and R.J. Yelf, 2003. Applications of GPR to surface mining. Proceedings of the 2nd international workshop on advanced ground penetrating radar, May 14 – 16, 2003, University of Technology, Delft, the Netherlands, pp: 115 – 119.

[10] D. Gomez-Ortiz, T. Martin – Crespo, S. Martin – Velazquez, P. Martinez – Pagan, H. Higueras, and M. Manzano, 2010. Application of ground penetrating radar to delineate clay layers in wetlands. A case study in the Soto Grande and Soto Chico watercourses, Donana (SW Spain). Journal of applied geophysics 72 (2010) 107 – 113.

[11] H.E. Gill, 1969. A groundwater reconnaissance of the republic of Ghana, with a description of geohydrologic provinces. US geological survey water – supply Pp 1757 – K, Washington, DC.

[12] N. Ismail Azwin, S. Rosli, M. Muztaza Nordiana, and A.H.A. The Saufia, 2012. A study of water table and subsurface using 3-Dimensional ground penetrating radar. International journal of environmental science and development, vol. 3, No. 6, December 2012.

[13] H.M. Jol 2009. Ground penetrating radar theory and applications. Elsevier science, Pp 12-24. ISBN: 978-0444-53348-7

[14] G.O. Kesse, 1985. The mineral and rock resources of Ghana. A.A Balkana, Rotterdam, Netherlands. ISBN – 13: 978 – 9061915973.

[15] J. Kevin Cunningham, 2004. Application of ground penetrating radar, digital optical borehole images, and cores for characterization of porosity hydraulic conductivity and paleokarst in the Biscayne aquifer, Southeastern Florida, USA. Journal of applied geophysics 55 (2004) 61 – 76.

[16] R. Knight, 2001. Ground penetrating radar for environmental applications. Annual review earth planet science 29: 229 - 55.

[17] W.M. Last, and J.P. Smaol, 2001. Tracking change using Lake sediments: physical and chemical techniques, Kluwer academic publishers, Dordrecht, The Netherlands.

[18] G. Leucci, 2006. Contribution of ground penetrating radar and electrical resistivity tomography to identify the cavity and fractures under the main church in Botrugno (Leucci, Italy). Journal of Archaeology science, 33:1194–1204.

[19] E. Manu, K. Preko, and D.D. Wemegah, 2013. Application of ground penetrating radar in delineating zones of gold mineralization at the Subenso-north concession of Newmont Ghana gold limited. International journal of scientific and research publications, volume 3, issue 5, Pp 6 -10, May 2013. ISSN2250 – 3153.

[20] T.P. Maria Peri and C. Giorgio, 2008. Hydrogeophysical methods for the dynamic characterization of hydrogeological systems. Scuola di Dottorato in Scienze della Terra, Dipartimento di Geo – scienze, universita studi di padova – A.A. 2008 – 2009.

[21] B. Milan Jr, and F.P. Haeni, 1991. Application of ground penetrating radar methods in hydrogeologic studies, vol. 29, No. 3 – groundwater – May – June 1991.

[22] Ming-Chih Lin, Yu-Ming Kang, Kun-Fa Lee and Hui-Chi Hsu, 2009. A study on the technologies for detecting underground water level and processing image. International journal of applied science and engineering 2009. 7, 1: 61 – 68.

[23] Nur Aswin Ismail and Rosli Saad, 2012. A case study on ground subsidence using ground penetrating radar. 2012 international conference on Environmental, Biomedical and Biotechnology, IPCBEE vol. 41 IACSIT press, Singapore.

[24] G.E. Omolaiye, E.A. Ayolabi, I. Ololade and C. Unuevho, 2011. Mapping the depth to groundwater using ground penetrating radar (GPR) in an oil producing community of western Niger Delta. The electronic journal of the international association for environmental hydrology. Vol. 19, pp 22.Overmereen Van, R.A., 1994. Georadar for hydrogeology, first break vol. 12 No. 8, August 1994/401

[25] J.E. Patterson, and F.A. Cook, 1999. Successful application of ground penetrating radar in the exploration of Gem Tourmaline (abstract) Canadian mineralogist, 37, p. 860 – 863

[26] J.A. Pilon, H.J.A. Russel, T.A. Bennand, D.R. Sharpe, and P.J. Barnett, 1994. Ground penetrating radar in a hydrogeological investigation of the Oak ridges Moraine, Ontario. Fith international conference on ground penetrating radar, Kitchener, Ontario, Cannada, vol. 2 of 3

[27] K. Preko, A. Scheuermann, and H. Wilhelm, 2009. Comparison of invasive and non-inovasive electromagnetic methods in soil water content estimation of a dike model. Journal of Geophysics and Engineering Vol 6 pp. 1-16.

[28] K. Preko, and H. Wilhelm, 2012. Detection of water content inhomogeneities in a dike model using invasive GPR guided wave sounding and TRIME-TDRR technique. Journal of Geophysics and Engineering Vol. 9, pp.1–15.

[29] S.K. Sandberg,, L.D. Slater, and R. Versteeg, 2002. An integrated geophysical investigation of the hydrogeology of an anisotropic unconfined aquifer. Journal of hydrology 267 &2002) 227 – 243.

[30] K.J. Sandmeier, 2012. The 2D processing and 2D/3D interpretation software for GPR, reflection Seismic and refraction seismic. Software catalogue 2012, Karlsruhe, Germany. http://www.sandmeier-geo.de/.

[31] S.F. Shih, J.A. Doolittle, D.L. Myhre and G.W. Schellentrager, 1986. Using radar for groundwater investigation. Journal of irrigation and drainage engineering 112920, 110 – 118

[32] K.K.K. Singh, 2006. Application of ground penetrating radar for hydro-geological study. Journal of scientific and industrial research, vol. 65, February 2006, pp. 160 – 164, central mining research institute, Dhanbad 826001.

[33] L. Slater, and T.M. Niemi, 2003. Ground-penetrating radar investigation of active faults along the Dead Sea Transform and implications for seismic hazards within the city of Aqaba, Jordan. Tectonophysics, 368: 33–50.

[34] A. Thomas Iivari and J.A. Doolittle, 1994. Computer simulations of depths to water table using ground penetrating radar in topographically diverse terrains. Groundwater quality management (Proceedings of the GQM 93 conference held at Tallinm, September 19973). IAHS publ. No. 220, 1994.

[35] P. Ulriksen, 1982. Application of impulse radar to civil engineering. Ph.D. Thesis, Department of Civil Engineering Geology, University of Technology, Lund, Sweden.

[36] Umar H., Mohd A. Ismail and Abdul R.S., 2008. Geophysical techniques in the study of hydrocarbon – contaminated soil. Bulletin of the Geological Society of Malaysia 54 (2008) 133 – 138, doi: 10. 7186/bgsm 2008020.

[37] Z. Ziaqiang, H. Zianqi, L. Guangyin, L. Qunyi, and L. Jianhui L, 2009. Ground penetrating radar exploration for ground water and contamination. PIERS proceedings, Moscow, Russia August 18 – 21, 2009

AUTHORS

First Author – Mr. E. Manu, MSc Geophysics, Research Scientist, Water Research Institute, CSIR, Ghana. Email: evans.manu2@gmail.com, evans.manutel@yahoo.com, Tel.: +233-202255630/243367930

Second Author – Dr. K. Preko, PhD Geophysics, Senior Lecturer, Department of Physics, Geophysics Unit, Kwame Nkrumah University of Science and Technology (KNUST), University Post Office, PMB, Kumasi Ghana. Email: kpreko@yahoo.com, kwasipreko.sci@knust.edu.gh. Tel: +233-242026899

Third Author – Mr. D.D. Wemegah, MSc Geophysics, Lecturer, Department of Physics, Geophysics Unit, Kwame Nkrumah University of Science and Technology (KNUST), University Post Office, PMB, Kumasi Ghana. Email: wemegah2@yahoo.co.uk. Tel.: +233-243477467, +244-260808054

Corresponding author- Mr. E. Manu, MSc Geophysics, Research Scientist, Water Research Institute, CSIR, Ghana. Email: evans.manu2@gmail.com, evans.manutel@yahoo.com, Tel.: +233-202255630/243367930